A diagnostic study of tropospheric diabatic heating and the generation of available potential energy

By JOHN A. BROWN, Jr., *National Center for Atmospheric Research, Boulder, Colorado*

(Manuscript received October 28, 1963)

ABSTRACT

Calculations of the horizontal distribution of mid-tropospheric diabatic heating have been made through use of the first law of thermodynamics in conjunction with a simplified form of the vorticity equation. Objective analyses of the geopotential heights of the 850 and 500 mb surfaces over a region extending from the pole southward to approximately 15° N were utilized. Calculations of the daily distributions of the heat sources and sinks were obtained for the following months: January 1959, 1962, 1963; April 1961, 1962; July 1961, 1962; and October 1961, 1962. The daily distributions were then averaged within each month, and one of the resulting monthly distributions for each season is presented. Furthermore, the 9 monthly averaged zonal heating profiles are presented together with the latitudinal variation of the heat flux required to maintain these profiles.

The zonal and eddy components of the generation of available potential energy were computed from the daily 500–850 mb thickness and heating patterns. The averaged zonal profiles of each component for each of the 9 months is presented. Furthermore, through a linear Fourier analysis method the eddy generation of available potential energy was obtained in the wave-number regime. The average monthly contribution and the standard deviation of the daily values were obtained for each of the 9 months for each harmonic from $n=1$ to $n=20$.

The results of the monthly averaged heating patterns indicate that relatively intense heat sources and sinks exist during the winter months while the least intense ones exist in the summer months. An annual zonal heating maximum of 4×10^{-3} kj t^{-1} sec^{-1} was found near 40° N and intense cooling existed in the high latitudes. All monthly averaged values of the zonal generation of available potential energy were positive with maximum values obtained for the winter months and minimum values obtained for the summer months. Results indicate that for the troposphere the available potential energy is generally destroyed by the eddies in all seasons except summer with the greatest destructions occurring in winter. Also, during winter the long waves, $n=1$ to 5, are responsible for the majority of this destruction. The annual average of the zonal generation of available potential energy for the troposphere obtained from the 9 months considered here was $+19 \times 10^{-4}$ kj m^{-2} sec^{-1} and the corresponding value for the eddy generation was -9×10^{-4} kj m^{-2} sec^{-1}.

1. Introduction

During past years investigations have been made which point to the importance of diabatic heating effects on atmospheric circulations. These effects and the corresponding generation of available potential energy are vital aspects in the study of the general circulation of the atmosphere.

This investigation is primarily an extension of an earlier one by Wiin-Nielsen & Brown (1960) in which results of diagnostic computations from daily height analyses of 850 and 500 mb data for January 1959 were presented. In this earlier study the heating fields and the generation of available potential energy were discussed in detail, and it was found that the results compared favorably with independent results obtained by some of the previous investigators. Thus, it was felt that the results were sufficiently encouraging to further pursue the question in order to obtain results which would reflect estimates of seasonal and annual variations. To obtain sufficient reliability in the results for the latter, of course, would require an enormous number of calculations.

In the present study results will be presented which were obtained from objective analyses of daily northern hemisphere data for April 1961, July 1961, October 1961, January 1962, April 1962, July 1962, October 1962 and January 1963. These, together with January 1959, form slightly more than two years of data consisting of calculations for a representative month from each of the four seasons.

A brief description of the atmospheric model which was employed in obtaining the daily heating fields is given in Section 2, together with the equations used to obtain estimates of the generation of zonal and eddy available potential energy. Furthermore, the formulations employed in obtaining the eddy forms in the wave number regime are also presented. Section 3 contains a brief description of the heating fields obtained and the resulting generation of available potential energy. An attempt to give a qualitative evaluation of the results is presented in Section 4.

Some of the calculations were performed on the IBM 709, but for the majority the IBM 7090 was utilized.

2. Method of calculation

(a) The model

A two-parameter quasi-geostrophic model similar to the one described by Wiin-Nielsen & Brown (1960) was used to obtain the daily heating fields. The primary difference between the present model and the one employed earlier was in the method of handling the lower boundary condition. Here an attempt has been made to incorporate frictional and terrain effects. Although the magnitude of such effects on the heating patterns may be small, it was believed that systematic influences might magnify the importance of such phenomena. The method of estimating these effects is basically the same as that presently used in short range numerical forecasting models of the National Meteorological Center and has been described in detail by Cressman (1959). Because of this the diagnostic method of calculation need only be described in brief.

The thermodynamic equation is applied at the 400–800 mb layer.

$$\frac{1}{c_p}\frac{dQ}{dt} = \frac{3}{2}\frac{g}{R}\left[\frac{\partial h}{\partial t} + \mathbf{V}\cdot\nabla h\right] - \frac{3}{2}\frac{P}{R}\sigma\omega, \quad (2.1)$$

where $$\sigma = -\alpha\frac{\partial ln\Theta}{\partial p}.$$

Here c_p is the specific heat at constant pressure, dQ/dt is the diabatic heating rate per unit mass, g is the acceleration of gravity, R is the gas constant, h is the 400–800 mb geopotential thickness, $\mathbf{V}$ is the mean horizontal wind in the layer, P is 400 mb, $\omega = dp/dt$ is the pressure vertical velocity, α is the specific volume, and θ is the potential temperature.

In order to obtain the heating we must first obtain an expression for ω. To do this we turn to the vorticity equation in the following form:

$$\frac{\partial\zeta}{\partial t} + \mathbf{V}\cdot\nabla(\zeta + f) = f_0\frac{\partial\omega}{\partial p}. \quad (2.2)$$

ζ is the vertical component of the relative vorticity, f is the Coriolis parameter, and f_0 is the Coriolis parameter at 45° N. Equation (2.2) is applied at 400 mb and 800 mb.

It is assumed that the vertical velocity vanishes at 200 mb. At the lower boundary

$$\omega = \omega_m + \omega_f, \quad (2.3)$$

where $$\omega_m = \mathbf{V}_g\cdot\nabla p_g \quad (2.4)$$

and

$$\omega_f = \frac{g}{\alpha f_0}\left[\frac{\partial}{\partial y}C_d(u^2+v^2)^{\frac{1}{2}}u - \frac{\partial}{\partial x}C_d(u^2+v^2)^{\frac{1}{2}}v\right]. \quad (2.5)$$

The subscript g refers to the quantity at the ground. The values of the skin drag coefficients, C_d, which were used were those introduced by Cressman (1960). The values of p_g were taken from the report by Berkofsky & Bertoni (1955). The x and y wind components at p_g are represented by u and v respectively. Equation (2.4) represents the vertical air motions induced by the terrain configurations, and (2.5) represents those due to the surface stress.

To obtain the wind near p_g a linear variation of the wind with respect to pressure was assumed. Furthermore, the geostrophic approximation was used throughout the formulation and the variation of static stability, although possibly important, was ignored. σ was set equal to 1.82 $m^3\,t^{-1}\,cb^{-1}$.

Thus equations (2.1) and (2.2) together with the above mentioned boundary conditions form a closed set of equations which were used to calculate the fields of diabatic heating, $1/c_p\ dQ/dt$.

The data which were used were the objective height analyses produced routinely by the National Meteorological Center at Suitland, Maryland. The method of analysis has been described by CRESSMAN (1959).

A twelve-hour time step was used in this study. This was dictated by the frequency at which upper air observations are made on a hemispheric scale. In addition to this, another requirement, which stems from the method of calculating the generation of available potential energy, was that the valid time (t) of the calculated heating fields should be reasonably close to the valid time of the thickness fields. In order to satisfy this latter requirement, it was decided to average in time the height fields at $t-12$ hrs and t hrs. The second set of data was next obtained by averaging the heights at t hrs and $t+12$ hrs. The resulting two sets of data were used as input to the model described. A second method of time differencing was tested on January 1962 data and will be described in Section 4.

Through use of finite difference techniques, fields of diabatic temperature changes were obtained at 0000 GMT and 1200 GMT for each day of each month studied. The data were obtained and the calculations were performed on the regularly arrayed 1977-point octagonal grid presently in use at the National Meteorological Center. The grid spacing is 381 km at 60° N on a polar sterographic projection. The equations described above were appropriately mapped. Thus the heating obtained represents that which is due primarily to large scale (a) latent heat of condensation or evaporation (or sublimation), (b) radiation and (c) turbulent exchange with the earth's surface.

It should be mentioned here that in addition to the errors which may be present due to the assumptions made in the modeling procedure, considerable errors may also be introduced into the individual calculations through analysis errors. Although the procedure presented here is admittedly sensitive to such errors, it is believed that such problems may be overcome to some extent by considering a sufficiently large number of cases. Of course if systematic errors exist, these will be damaging to the final result. The extent of such difficulties may be qualitatively assessed by comparison with independent calculations.

(b) THE GENERATION OF AVAILABLE POTENTIAL ENERGY

The concept of available potential energy was originally introduced by MARGULES (1903) and has been described in considerable detail by LORENZ (1955). It has been defined as the portion of the potential and internal energy (total potential energy) which is available for conversion into kinetic energy, and is equal to that amount of total potential energy which would be released if the mass of the atmosphere was rearranged under isentropic changes in such a way as to result in horizontal isentropic surfaces with stable stratification. Furthermore, Lorenz has shown that the generation of available potential energy is dependent upon the volume integral of the product of the deviations of the diabatic heating and the temperature from the area average of these quantities. Thus, approximately

$$G_A = -\frac{R}{\sigma c_p}\int_0^{p_0}\int_s \frac{1}{p}\left(\frac{\partial z}{\partial p}\right)'\left(\frac{dQ}{dt}\right)' dS\,dp. \quad (2.6)$$

Here z is the geopotential height of an isobaric surface, S denotes the area over which the integration is to be performed and p_0 is the mean surface pressure and has been set equal to 1000 mb. Also

$$(\ )' = (\ ) - \overline{(\ )}, \quad (2.7)$$

where

$$\overline{(\ )} = \frac{1}{S}\int_s (\ )\,dS \quad (2.8)$$

is the area average. It can be seen from equation (2.6) that available potential energy is generated when warm air is heated and cold air is cooled.

Next we introduce the concept of zonal available potential energy and eddy available potential energy as described by Lorenz. If we define an average about a latitude circle as

$$\widetilde{(\ )} = \frac{1}{L}\int_L (\ )\,dx \quad (2.9)$$

where x is measured positively towards the east and L in the length of the latitude circle,

$$G_A = G_A^{(z)} + G_A^{(e)}. \quad (2.10)$$

Here

$$G_A^{(z)} = -\frac{R}{\sigma c_p}\int_0^{p_0}\int_s \frac{1}{p}\widetilde{\left(\frac{\partial z}{\partial p}\right)'}\widetilde{\left(\frac{dQ}{dt}\right)'} dS\,dp \quad (2.11)$$

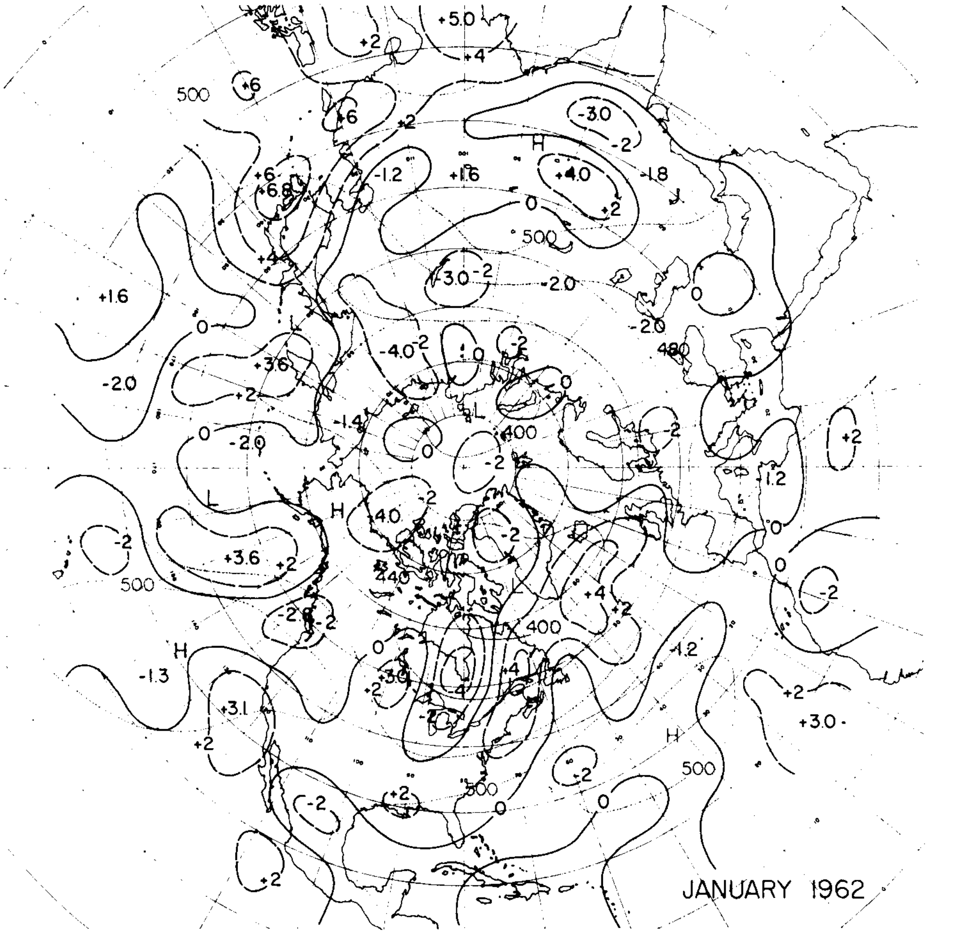

Fig. 1 *a*.

and

$$G_A^{(e)} = -\frac{R}{\sigma c_p}\int_0^{p_0}\int_S \frac{1}{p}\left(\frac{\partial z}{\partial p}\right)''\left(\frac{dQ}{dt}\right)'' dS\,dp, \quad (2.12)$$

where

$$(\ )' = \widetilde{(\ )'} + (\ )''. \quad (2.13)$$

Thus the single prime denotes the deviation from the area average and the double prime denotes the deviation of this quantity from the average value about a latitude circle. The contribution by the area averaged terms has been ignored.

Since $\partial z/\partial p$ can be approximated from observed heights and the calculations described in the previous section give estimates of the heating field, it is possible to calculate the generation of zonal available potential energy, $G_A^{(z)}$, and the eddy available potential energy, $G_A^{(e)}$, for the atmospheric layer. Since it has been assumed that ω vanishes at 200 mb, the effective depth has been considered to extend from the surface to 200 mb. Notice that in the definition of the available potential energy the stability, σ, has been treated as a constant here also—3.0 $m^3\ t^{-1}\ cb^{-1}$.

(c) The generation of eddy available potential energy in the wave number regime

As will be seen in the following section, equation (2.12) was evaluated over the region of interest and furthermore expressed as a function of latitude. However, it is also of interest to

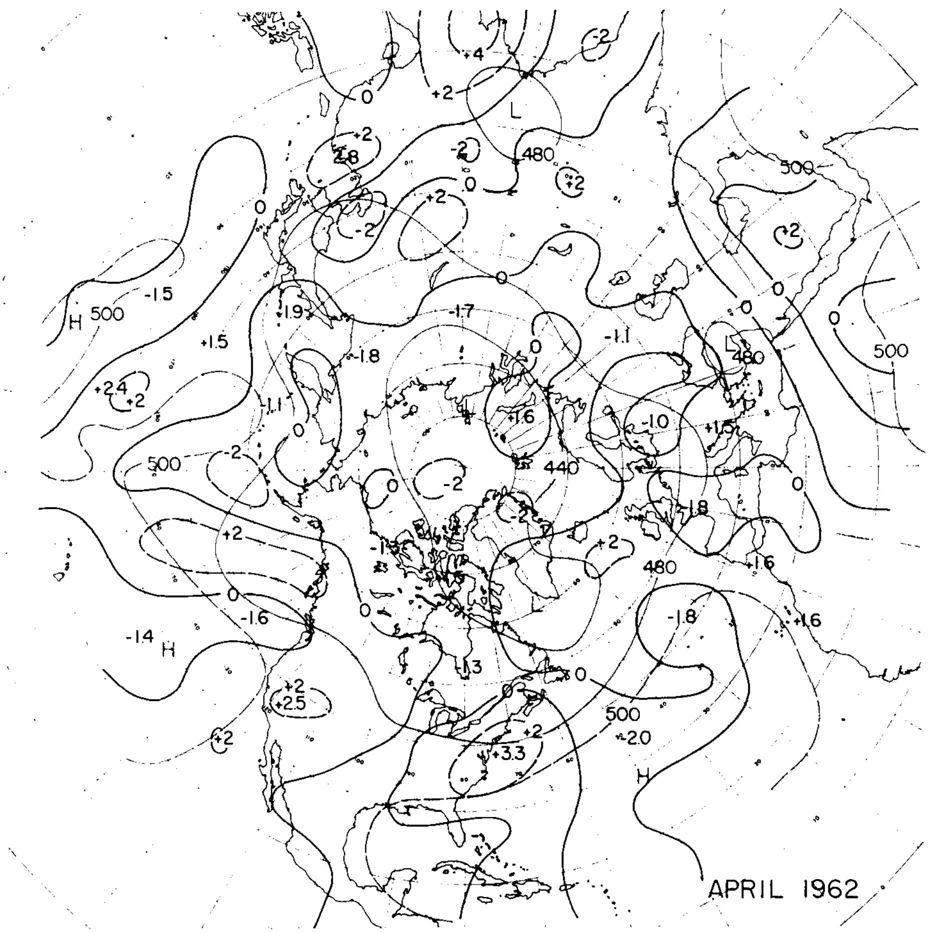

Fig. 1 *b*.

determine $G_A^{(e)}$ over the wave number spectrum in order to determine the distribution of the eddy generation over the various scales of atmospheric motion. The results of such calculations will show whether the eddy generation is equally distributed over the entire spectrum (or parts thereof), or whether certain scales of motion are preferred for large amounts of generation or destruction.

The method which was used was analogous to the one employed by WIIN-NIELSEN (1959) in obtaining the conversion between potential and kinetic energy. Also since the method in the present investigation is similar to one described by WIIN-NIELSEN & BROWN (1960), the reader is referred to these reports for the detailed description of the procedure.

Linear Fourier analyses were made on the 500–850 mb daily analyses and the corresponding computed heating fields. The grid point values which were available in the regular array of the octagonal grid were first interpolated quadratically to latitude-longitude intervals of 2.5°. One-dimensional Fourier analyses were made about each latitude circle using the available 144 values. The method used here differed slightly from the one used previously, since here the analyses were made using interpolated values at the latitude circles, while the previous electronic computer program was designed to utilize the regularly arrayed values and perform the linear Fourier analysis in bands with a width of one grid increment.

The results of the method employed gave the

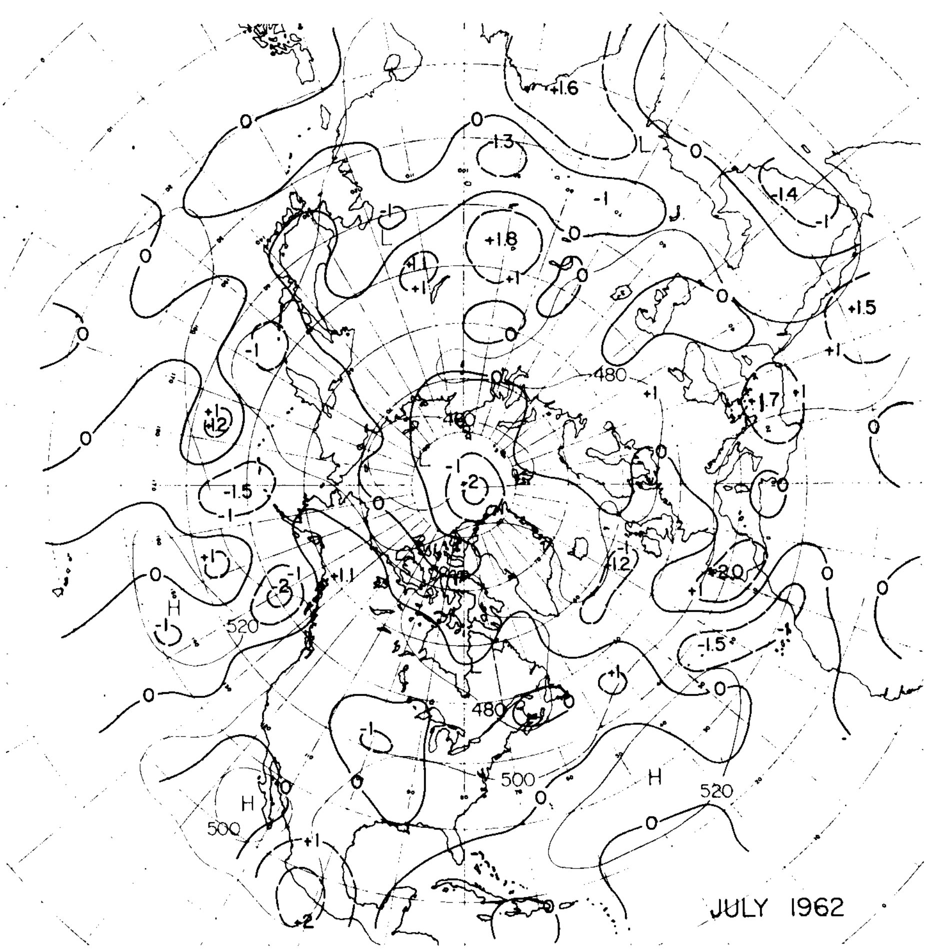

Fig. 1 c.

zonal available potential energy, G_{A0}, from wave number $n=0$ and the generations, G_{An}, corresponding to wave number $1 \leqslant n \leqslant 20$. Thus

$$G_{A0}(\varphi) = 2k^* \int_{\varphi_0}^{\varphi_1} a_0 A_0 \cos\varphi d\varphi, \quad (2.14)$$

$$G_{An}(\varphi) = k^* \int_{\varphi_0}^{\varphi_1} (a_n A_n + b_n B_n) \cos\varphi d\varphi. \quad (2.15)$$

In these equations $\varphi_1 = 87.5°$ N and $\varphi_0 = 20.0°$ N. The Fourier coefficients for the 500–850 mb thickness field and the heating field are denoted by a_n, b_n and A_n, B_n. k^* is the constant of proportionality for the effective depth considered. Notice that

$$G_{A0} = G_A^{(z)}. \quad (2.16)$$

Equations (2.14) and (2.15) were solved using the 0000 GMT and 1200 GMT daily values, and the standard deviation of each G_{An} was computed for each month.

3. Results

(a) Average monthly patterns

The atmospheric model which was described in Section 2*a* was used to calculate the heating patterns for each map-time and then the results for a given month were averaged. To eliminate the less important small scale features, a linear Fourier analysis was performed on the resulting field for every 5 degrees of latitude and longitude and the resulting sum of the first 15 harmonics plus the zonal component in units of degrees Kelvin per day are presented for four months

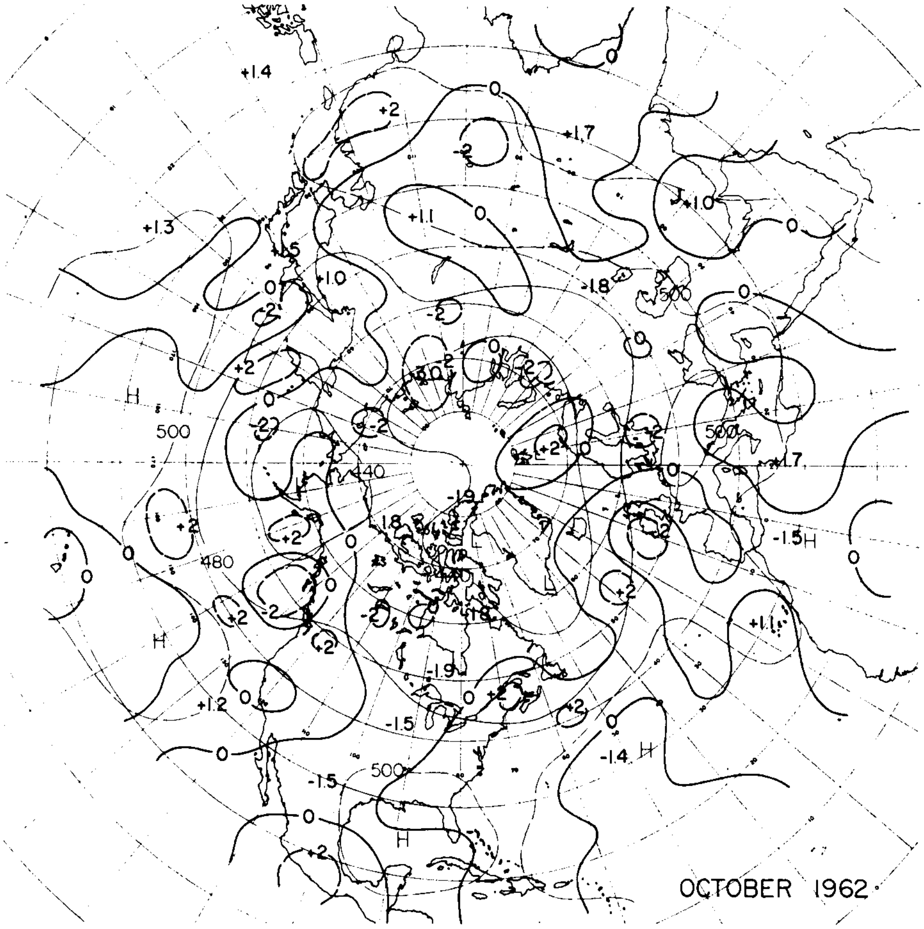

Fig. 1 *d*.

FIG. 1. (*a*) Average monthly distribution of $(1/c_p)\ (dQ/dt)$ for the 400–800 mb layer in units of degrees Kelvin day^{-1} for January 1962. The average 850 mb contours in deca feet are superimposed in red. (*b*): As (*a*) but for April 1962. (*c*): As (*a*) but for July 1962. (*d*): As (*a*) but for October 1962.

in Fig. 1. The mean 850 mb contours obtained from the daily height analyses are superimposed onto the mean heating fields in order to give an indication of the average monthly synoptic pattern.

Intense heat sources and sinks were found during the winter months, while minimum heating activity resulted in the summer months. The arctic region was found to be a strong heat sink in winter. Preferred heat source regions appeared near the eastern coasts of Asia and North America, and in the Gulf of Alaska. The heating near the coast of North America in January 1959 was found further east than that which resulted in the other January months. This coincides with the fact that the mean position of the 850 mb trough was also located further east. Of all months considered, the most intense heat source occurred in January 1963 off the east coast of Asia. It was about twice the intensity of that found in January 1962. Extreme abnormalities of the hemispheric circulation existed in this month.

Many of the major features in the heating patterns which resulted from the calculations in winter were also evident to a lesser degree in the spring and fall months. However many differences in the details of the configurations can also be found from one season to the next and from the same season of one year to the same

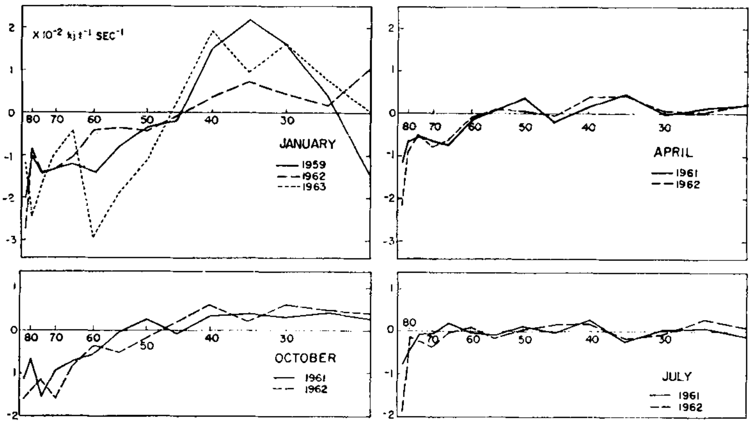

FIG. 2. Zonal averages of the mean monthly heating for the 400–800 mb layer in units of 10^{-2} kj t^{-1} sec^{-1} (ordinate) plotted as a function of the sine of latitude (abscissa).

season of the next year. The magnitude of the heating in July is significantly less than that found during the other seasonal months.

(b) THE MEAN HEATING AS A FUNCTION OF LATITUDE AND THE STEADY STATE MERIDIONAL HEAT FLUX

The meridional distributions of the calculated diabatic heating were obtained from the averaged heating fields. These were obtained from the corresponding mean fields of diabatic heating for the months by computing the averaged values along latitude circles. The area average of the heating for a particular month as obtained in this study is proportional to the area average of the local thickness tendencies and furthermore depends upon the net inflow into (or outflow from) the region under consideration. Because of the modeling approximations which have been made, it is felt that the net heating obtained here is meaningless. Therefore this has been set equal to zero and the resulting meridional distributions are plotted in Fig. 2 against the sine function of the latitude in order that a unit of distance on the abscissa may represent a fixed area of the earth. It was found that the results obtained from the calculations for January 1959 which did not incorporate the terrain and frictional effects (not shown) differed little from those which included these effects, except near the boundary of the region where the lateral boundary approximations and analysis inaccuracies are believed to be damaging.

From Fig. 2 it can be seen that for the January calculations atmospheric cooling is observed on the average in all latitudes down to about 45° N and intense heating occurs further southward. In this latter feature maxima of 2.2×10^{-2} kj t^{-1} sec^{-1} at 35° N in January 1959 and 1.9×10^{-2} kj t^{-1} sec^{-1} at 40° N in January 1963 may be compared with 0.7×10^{-2} kj t^{-1} sec^{-1} at 35° N for January 1962. In both the April months considered, it can be seen that the atmospheric cooling extends down to approximately 60° N latitude, which is considerably further north than was observed in the January months. Both of the April months have features which are very similar. A secondary heating maximum occurs between 60° N and 45° N with a primary maximum of approximately 0.5×10^{-2} kj t^{-1} sec^{-1} at about 35° N. During the July months the magnitudes of the average meridional heating are considerably smaller than those observed in the winter and spring months. Furthermore, regions of warming extend into higher latitudes. In October the cooling regions recede southward again and extend down to the upper mid-latitudes.

A comparison of the seasonal patterns reveals intense atmospheric heating and cooling in the winter months, diminishing somewhat in the spring months, reaching a minimum of activity in the summer months, and then intensifying again during the fall.

If we assume for the moment that the heating distribution as obtained for a particular month

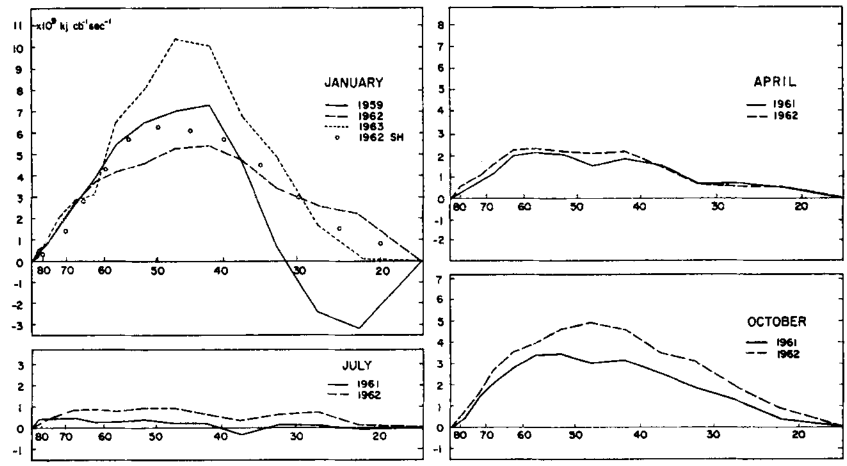

FIG. 3. Monthly averages of the meridional heat flux in units of 10^9 kj cb^{-1} sec^{-1} (ordinate) plotted against the sine of the latitude (abscissa). The circles (upper left) represent the sensible heat flux values obtained by Wiin-Nielsen, Brown and Drake for January 1962.

is a steady state condition, an estimate of the meridional heat flux, F, necessary to maintain this state can be obtained. In spherical coordinates the meridional heat flux gradient is

$$\frac{dF}{rd\varphi} = \int_0^\infty \frac{2\pi r}{\alpha} \cos\varphi \widetilde{\left(\frac{dQ}{dt}\right)'} dz$$

$$= \frac{1}{g}\int_0^{p_0} 2\pi r \cos\varphi \widetilde{\left(\frac{dQ}{dt}\right)'} dp. \quad (3.1)$$

Here r is the mean earth radius. Thus

$$F = \frac{2\pi r^2}{g}\int_{\pi/2}^{\varphi} \cos\varphi \widetilde{\left(\frac{dQ}{dt}\right)'} d\varphi. \quad (3.2)$$

Since $F = 0$ near the pole, equation 3.2 can be used to obtain the flux in units of kj cb^{-1} sec^{-1} as a function of latitude.

The results of this calculation for the individual months are shown in Fig. 3. Positive values denote northward transports. As should be expected the maximum northward heat flux occurs in January, the minimum in July and amounts approximately midway between these in the spring and fall months. In all January months the maximum occurred near 45° N. The results for January 1959 in the lower latitudes differ considerably from those of the other years. The geostrophic sensible heat flux has been computed for the atmosphere for January 1962 by WIIN-NIELSEN, BROWN & DRAKE (1963) using the National Meteorological Center's daily objective height analyses at 850, 700, 500, 300 and 200 mb levels. The results for January 1962 are also presented in Fig. 3. Both methods have the inherent characteristic that requires the flux to vanish near 17.5° N. This requirement introduces errors into the result which could be significant particularly in the lower latitudes. Nevertheless a comparison of these results reveals that the steady state heating flux obtained in the present study can be interpreted as a close representation of the mean flux in the troposphere for January 1962 if the horizontal sensible heat flux is the major heat balancing parameter. The geostrophic sensible heat flux for January 1959 (not shown) was also computed using 850 and 500 mb data only. Again the sensible heat flux maximum in midlatitudes (9.4×10^9 kj cb^{-1} sec^{-1} at 45° N) was greater than the steady state flux maximum found in this study (7.3×10^9 kj cb^{-1} sec^{-1} at 42.5° N).[1] The sensible heat flux was negative south of 25° N, but these magnitudes were considerably smaller than those found in the present study.

From Fig. 3 it can be seen that the results of the sensible heat flux for the two April months

[1] The results obtained for January 1959 which did not incorporate the friction and mountain effects produced a steady state heat flux maximum near 40° N which was slightly greater than that obtained from the sensible heat flux calculation.

26 – 642898

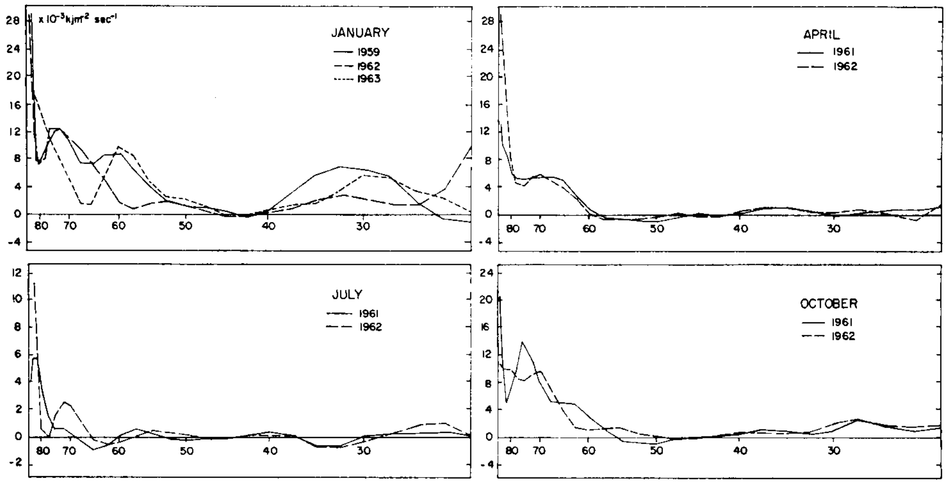

FIG. 4. Monthly mean of $G_A^{(z)}$ for the 1000-200 mb layer in units of 10^{-3} kj m^{-2} sec^{-1} (ordinate) versus the sine of latitude (abscissa).

are very similar. Both show northward heat flux at all latitudes with a primary maximum at 57.5° N and a secondary maximum at 42.5° N. These features are similar to those for October 1961, except that the magnitude of the flux is larger in October. The heat flux in the summer months is northward at almost all latitudes but is considerably less intense.

(c) THE ZONAL GENERATION OF AVAILABLE POTENTIAL ENERGY

The monthly average distributions of the generation of zonal available potential energy as a function of latitude were obtained from the daily calculations, and the results are shown in Fig. 4. The meter-ton-second system of units is again used. The most pronounced feature displayed by these diagrams is the positive values which occur at most latitudes during all seasons. Thus for the zonal average the atmosphere which is relatively warm in the lower latitudes is heated and that which is relatively cold in the higher latitudes is further cooled. It is believed that the large values in Fig. 4 which were obtained near 90° N are the result of averaging over a relatively small area.

In winter the zonal generation is very pronounced over northerly latitudes down to 55° or 60° N, small negative values (destruction) were obtained about 45° N, and large positive values resulted in the lower latitudes under consideration. From the January 1959 results it was found that the method of accounting for the effects of friction and mountains at the lower boundary of the model tends to produce smaller values locally (not shown), but does not alter the profile significantly. The average values for the various latitudes diminished considerably from January to April. A close inspection of the April months shows much similarity in the profiles. The trend for lesser zonal generations continues on into July where again noticeable similarities exist in the two profiles. (Notice that the ordinate has been magnified for these profiles.) The trend reverses itself from July to October where again we see pronounced generations occurring, particularly at the higher latitudes. Again we see that the October 1961 and October 1962 profiles bear significant resemblances.

As was mentioned previously, the stability, σ, was treated as a constant. A value of $\sigma = 1.65$ m^3 t^{-1} cb^{-1} was tested on the July 1962 data in order to see what effects would result by using a seasonal value rather than an annual one. It was found that the results differed very little from the previous ones, and therefore seasonal variations of this parameter accounted for in this manner could be ignored.

In the January months which were considered in this study the daily values of the total zonal generation of available potential energy were very seldom negative. For example, in January 1962 the total zonal generation for the

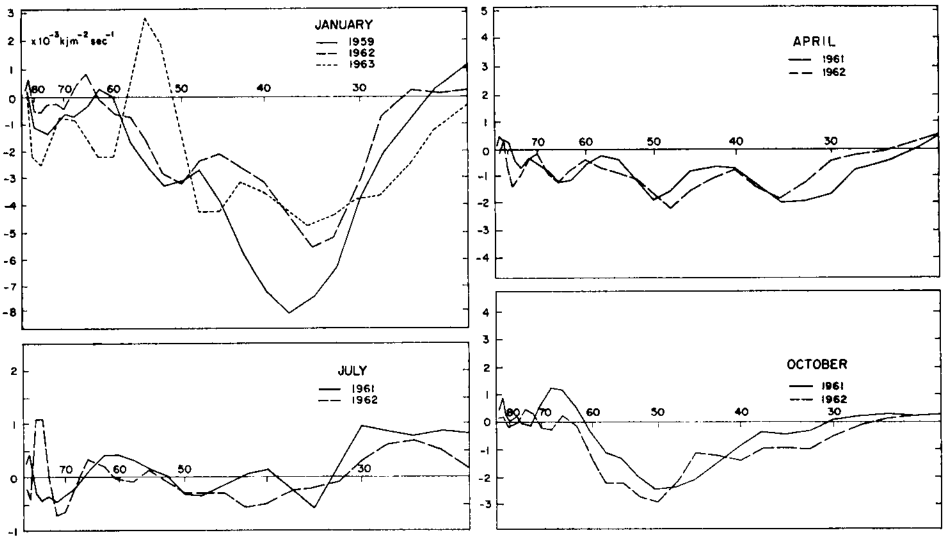

FIG. 5. Monthly mean of $G_A^{(e)}$ for the 1000-200 mb layer in units of 10^{-3} kj m^{-2} sec^{-1} (ordinate) versus the sine of latitude (abscissa).

area north of about 20° N was positive in 58 calculations out of the 60 which were performed. The magnitudes of the two calculations which were negative (0000 GMT 6 January and 1200 GMT 18 January) were extremely small in relation to the majority of the positive values. The number of daily results showing a destruction of zonal available potential energy were greater in the April and October months with a maximum occurring in the July months. In July 1962 there were 17 out of the 60 calculations showing negative values. Of course the magnitudes of the total zonal generations were considerably smaller for these summer months.

(*d*) THE EDDY GENERATION OF AVAILABLE POTENTIAL ENERGY

Calculations have been made from the daily 500–850 mb thickness and heating fields of the eddy generation of available potential energy through use of equation (2.12). These results have been averaged for the individual months and are shown in Fig. 5 as a function of latitude. Again it was found that the effect of including the mountain and friction terms produced smaller values locally but did not significantly alter the January 1959 profile.

From the results shown in Fig. 5 we see that considerably large destructions of eddy available potential energy occur over large regions during the seasons which are dynamically active. These results indicate that on the average there is a tendency for cold eddies to be warmed and warm eddies to be cooled. We note that this is a very pronounced feature in the January months in mid-latitudes. Notice also that the large minimum values are shifted to higher latitudes in October. The large minimum found near 35° N in January is significantly weaker in April while the secondary minimum found near 50° N in January 1959 and 1962 is only slightly weaker in April. January 1963 differed from the other winter months in several major respects. The destruction by the eddies was more pronounced in the northern latitudes down to 60° N, large generations resulted between 50° N and 60° N, and the eddy destruction between 20° N and 30° N was significantly greater. The magnitude of the eddy generations obtained for the July months was smaller than those obtained for the other months. (Notice that the ordinate has been magnified for these months.) Furthermore, the profiles here are more irregular. The most pronounced feature for these months is the relatively large positive values of the eddy generation which occur between 20° N and 30° N. Here also it was again found that the different stability value for July 1962 did not change the profile significantly (not shown).

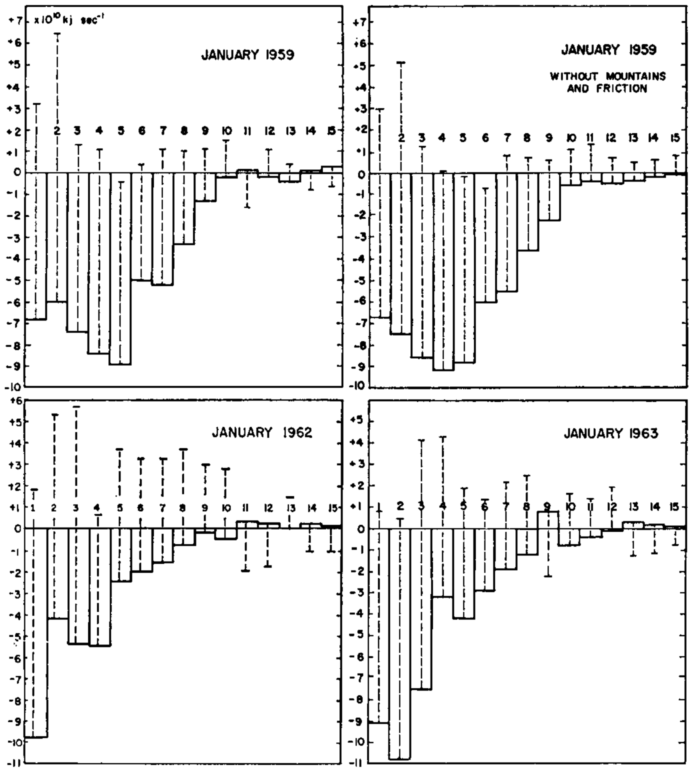

FIG. 6. January monthly means and standard deviations of G_{An} for $n = 1$ to $n = 15$ in units of 10^{10} kj sec^{-1} for the 1000-200 mb layer.

The method described in Section 2*c* above was employed to obtain the eddy generation as a function of wave number. The calculations were performed utilizing the daily heating and thickness fields, and the monthly averaged results are shown in Figs. 6, 7, 8 and 9. Values were obtained for $n = 1, 2, \dots 20$. However, magnitudes beyond $n = 15$ were very small. The blocks represent the generations in the mean for the month and the dashed lines represent the standard deviations of the daily average contributions. The results for January 1959 which were obtained from the diabatic heating model in which ω was set equal to zero at $p = 1000$ mb are presented here since a minor error has been found in the earlier results. However, the gross features remain unaltered. The units are 10^{10} kj sec^{-1}. Here we see that the mountain and friction effects tend to reduce the G_{An} values with the largest reduction observed for $n = 2$ and the smallest for $n = 1$ and $n = 5$. Thus the maximum destruction shifted from wave number 4 to

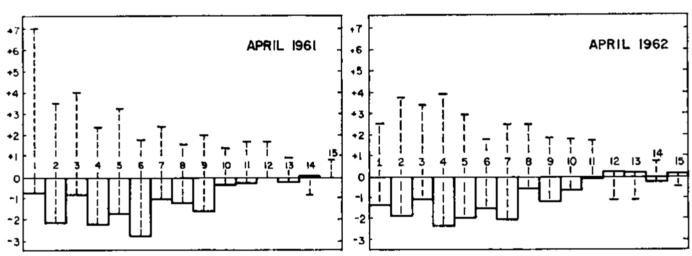

FIG. 7. As Figure 6 but for April months.

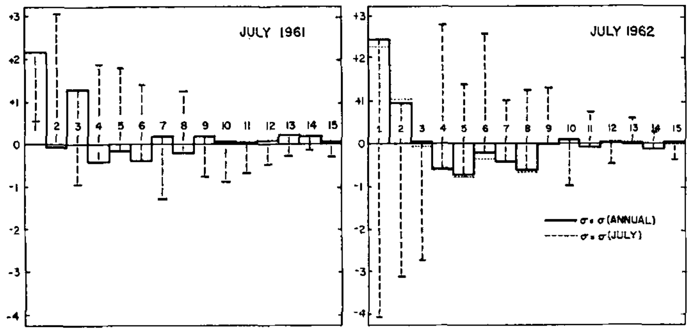

FIG. 8. As Figure 6 but for July months.

wave number 5. In the winter months we find that the destruction is most pronounced in the longer waves. From the standard deviations we see furthermore that positive generations occurred in many cases. In the spring months the eddy destruction is more evenly distributed over the spectrum from $n = 1$ to 10. In summer we find noticeable generations occurring in the small wave numbers. This is prevalent to some extent in October, but in addition we notice here an increasing destruction in the moderate wavelengths where baroclinic instabilities prevail. The dashed lines for July 1962 are the results obtained using the seasonal stability value. The values obtained for $n > 10$ were relatively small for all months.

(e) GENERATION OF AVAILABLE POTENTIAL ENERGY FROM MONTHLY AVERAGED FIELDS AND FROM STEADY STATE APPROXIMATIONS

The monthly averages of the zonal ($G_A^{(z)}$) and eddy ($G_A^{(e)}$) generation of available potential energy, obtained from the daily computations, are presented in columns D of Table 1. The results obtained in the previous study by WIIN-NIELSEN & BROWN (1960), in which ω was set equal to zero at the lower boundary, is shown in the first row of this table and denoted with an asterisk. Here we see that $G_A^{(z)}$ was 50×10^{-4} kj m^{-2} sec^{-1} and $G_A^{(e)}$ was -35×10^{-4} kj m^{-2} sec^{-1}. The results of the calculations show large magnitudes of the generation in winter, becoming smaller in spring, reaching minimum values in summer, and increasing again in fall. $G_A^{(e)}$ values are negative for all months except July where relatively small average eddy generations are found.

Values for $G_A^{(z)}$ and $G_A^{(e)}$ were also obtained, through the same method as described above, using the monthly averaged 850 mb heights, 500 mb heights and diabatic heating fields. The results are shown in columns M of Table 1. In other words, the values shown in columns D are the results of averaging the daily $G_A^{(z)}$ and $G_A^{(e)}$ values while the values in columns M are the $G_A^{(z)}$ and $G_A^{(e)}$ quantities obtained from the monthly averaged fields (standing part). Notice the extremely close correspondence of the zonal generation results and the large differences in the eddy generation results of the two procedures. Thus we see that the standing part can be used to closely approximate $G_A^{(z)}$, but cannot be used to obtain the monthly averages of $G_A^{(e)}$. These results indicate that the average daily

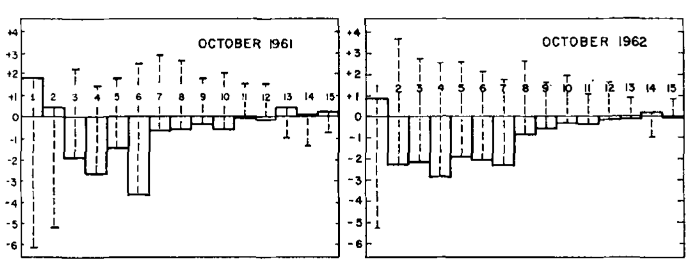

FIG. 9. As Figure 6 but for October months.

TABLE 1.

Month	$G_A^{(z)}$ D	$G_A^{(z)}$ M	$G_A^{(z)}$ SS	$G_A^{(e)}$ D	$G_A^{(e)}$ M	$G_A^{(e)}$ SS
January 1959*	50.0	48.0		−35.1	−7.4	
January 1959	43.0	47.2	4.1	−29.8	−6.5	−14.8
January 1962	35.0	36.1	17.7	−18.1	−5.6	−16.6
January 1963	35.6	39.4	28.9	−23.5	−12.2	−28.9
April 1961	13.8	13.5	−0.7	−8.6	0.2	−2.0
April 1962	14.6	14.7	1.3	−7.9	0.5	−2.6
July 1961	1.6	1.7	−0.6	2.0	2.4	1.1
July 1962	4.5	4.7	0.7	0.5	2.1	1.2
October 1961	22.1	22.2	2.3	−5.3	2.2	−3.0
October 1962	22.8	23.1	3.9	−8.6	0.5	−3.6

correlation of the meridional thickness and heating profiles is closely approximated by the correlation of the averaged profiles. This is substantiated by the fact that the meridional profiles of $G_A^{(z)}$ obtained from the second method (not shown) very closely resemble those shown in Fig. 4. However the transient eddies appear to be important in accounting for the total eddy generation.

A third method of computing the monthly averages of the available potential energy generations can be made if we assume a steady state condition. For a particular month it was assumed that the averaged 850 mb and 500 mb height patterns were steady state fields. The diabatic heating field was then obtained through use of the model described in Section 2*a*. The averaged zonal and eddy generations of available potential energy were then calculated. The results for the various months are shown in columns SS of Table 1. As can be readily seen, the results from such a procedure produce $G_A^{(z)}$ and $G_A^{(e)}$ values which differ greatly from those obtained from the average of the daily calculations.

4. Summary and qualitative assessment of results

In the past most diabatic heating diagnostic studies have been based on one of two fundamental methods: (1) direct estimates of condensation and evaporation, radiation, and conduction through turbulent exchange between the atmosphere and earth; (2) indirect estimates resulting through use of the first law of thermodynamics. This study is of the latter type. Of course both methods contain inherent weaknesses. The model which was employed in the present study is particularly sensitive to analysis errors and as a result the details of the calculation for a specific day may be erroneous. Although obtaining monthly averages of such calculations should minimize errors which are of such a random nature, one must be extremely cautious when interpreting results over regions of sparse data coverage.

Although the model which has been used here to obtain the fields of diabatic heating on a daily basis is a very simple one, favorable comparisons of results obtained by WIIN-NIELSEN and BROWN (1960) for January 1959 (using an even more simplified model) were beyond initial expectations and supported further pursuit. Thus eight additional months have been investigated in an attempt to obtain estimates of seasonal synoptic[1] variations of the tropospheric heating patterns and the corresponding generation of available potential energy.

The diabatic heating patterns presented in Fig. 1 consist of many details which are difficult to explain individually. However, from the gross features, we see that regions of atmospheric heating were obtained near the east coasts of Asia and North America for all months considered and were more pronounced in the colder seasons. Furthermore, cooling is pronounced north of about 50° N in the winter and fall months.

[1] Although the generation processes, which are of a smaller scale than the grid network used here, may be of importance on the global scale, an estimate of their contribution is beyond the scope of this investigation.

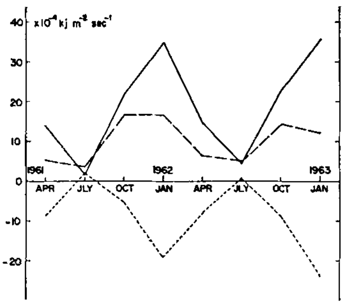

FIG. 10. The monthly averages of $G_A^{(z)}$ (solid line), $G_A^{(e)}$ (small dashed line) and $G_A^{(z)}+G_A^{(e)}$ (large dashed line) versus time. Units are 10^{-4} kj m^{-2} sec^{-1}.

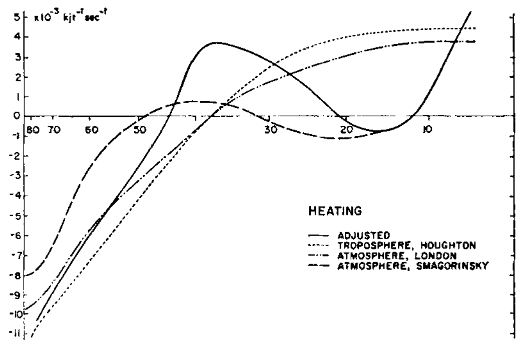

FIG. 12. Adjusted mean diabatic heating from present study (solid line), from Houghton (small dashed line), from London (dash-dotted line) and from Smagorinsky (large dashed line) plotted against the sine of latitude (abscissa). Units are 10^{-3} kj t^{-1} sec^{-1}.

The zonal and perturbation available potential energy was obtained from the daily 500–850 mb thickness and heating fields. The averages of these quantities for the seasonal months considered are plotted as a function of time and are shown in Fig. 10. For the consecutive months of the two-year period we see maximum magnitudes occurring in the winter months and minimum values in the summer. The average eddy available potential energy is approximately the same in spring and fall, but the zonal amounts for the fall are on the average 58 % larger than those calculated for spring. In summer both the eddy and zonal values are small and positive. Consequently we find maximum positive values of the total generations of available potential energy in the fall and winter months and minimum positive values in spring and summer.

The annual average of the diabatic heating as a function of latitude has been obtained from the nine months considered in this study. The resulting profile is shown in Fig. 11. Because of the restrictions dictated by the computational method and the degree of accuracy of the analyses, the net heating between the pole and 20° N has been set equal to zero. It can be seen that a maximum heating of 5×10^{-3} kj t^{-1} sec^{-1} was found near 40° N and maximum cooling in high latitudes.

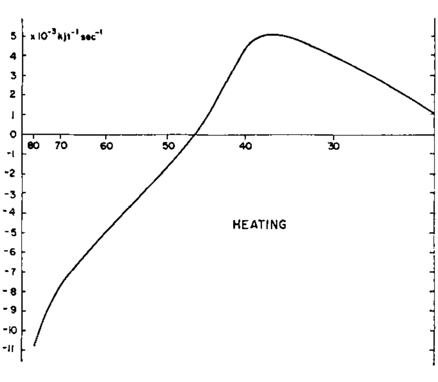

FIG. 11. Annual mean diabatic heating in units of 10^{-3} kj t^{-1} sec^{-1} (ordinate) plotted against the sine of latitude (abscissa).

The latitude variation of the annual diabatic heating should be more representative of the real profile if estimates of the heating south of 20° N were available. Such a profile has been deduced by SMAGORINSKY (1963) from LONDON's (1957) radiational balance and BUDYKO's (1956) heat balance at the earth's surface. The values obtained by Smagorinsky for the region south of 20° N have been used, and the heating profile obtained in the present study has been adjusted by setting the net heating from pole to equator equal to zero. The resulting profile is presented in Fig. 12 together with those obtained by HOUGHTON (1954), LONDON (1957), and SMAGORINSKY (1963). The results obtained by Houghton represent the annual mean of the net radiational heating at the tropopause while London's results are to be interpreted as the annual mean radiational balance at the top of the atmosphere. The differences in these results are also due largely to the differences in the methods of estimating the radiational components. The heat balance at the surface of the earth includes both latent and sensible heat exchanges. The profiles in Fig. 12 which were

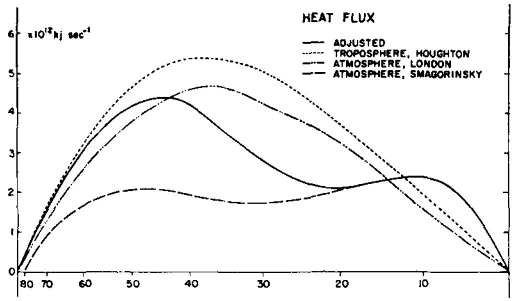

FIG. 13. Necessary heat flux required to balance diabatic heating curves of Figure 12 plotted against the sine of the latitude. Units are 10^{12} kj sec^{-1}.

obtained by the writer and the one obtained by Smagorinsky contain these latter processes. Considerable disagreement in these profiles can be noticed. It is difficult to determine how much of the differences might be attributed to abnormalities in the circulations of the particular months considered in the present study. The heating maximum found near 40° N in this study is 3.8×10^{-3} kj t^{-1} sec^{-1} while that deduced by Smagorinsky at 40° N is about 0.6×10^{-3} kj t^{-1} sec^{-1}. Furthermore, considerably larger cooling rates are found north of 45° N in the present study. A portion of these discrepancies are due to the fact that for this comparison we have assumed the heating of the present investigation to be representative of the entire atmosphere. Recently DAVIS (1963) has obtained estimates of the total heating from 20° N to 70° N in several layers from 1010 to 25 mb. His resulting measurements of the heating components indicate an annual net heating from 20° N to 60° N in the 1010 to 500 mb layer, but a thermal deficit was found generally when the 1010 to 25 mb layer was considered. Thus we must bear these general results in mind when we compare the results of the present investigation with others representative of the entire atmosphere.

The necessary heat flux required to balance the radiative gradients obtained by Houghton and London and that to balance the net heating obtained in this study and by Smagorinsky are given in Fig. 13. The radiative flux maxima obtained from the two latter investiga.ions occur at 40° N. In the present investigation the mean heating which was obtained in the layer between 800 and 400 mb was again assumed for convenience to be representative of the entire atmosphere. One should bear this in mind when comparisons of the profiles are made. An important difference to be noted is the relative size of the flux maxima near 45° N and 10° N which was obtained by Smagorinsky and the writer. Furthermore, the minimum found by Smagorinsky near 30° N is near 20° N in the present study.

SUOMI & SHEN (1963) have recently obtained estimates of the eddy generation of available potential energy due to terrestrial infrared radiation. Measurements from Explorer VII over a region in the western part of the northern hemisphere in mid-latitudes for several days in December 1959, February 1960 and April 1960 were utilized. An average value of $+5.8 \times 10^{-4}$ kj m^{-2} sec^{-1} was obtained. Thus in the case of the eddies the covariance of temperature and heating based on infrared radiation was positive. Thus, if we accept the negative covariances as obtained in the present study for January and April, then the configurations of the heating patterns due to other processes must outweight the effects attributable to infrared radiation alone.

Estimates of the zonal and eddy generation of available potential energy due to the total heating have been made by CLAPP (1961) using climatological data. The average heating between 1000 and 500 mb was obtained for January from estimates of condensation and evaporation, sensible heat exchange, and radiational processes. From the resulting normal heating field and the normal thickness field an average value of $+2.23 \times 10^{-4}$ kj m^{-2} sec^{-1} was obtained for the zonal available potential energy and $+3.82 \times 10^{-4}$ kj m^{-2} sec^{-1} was obtained for the eddy generation in the region from 30° N to 60° N. The zonal component is an order of magnitude smaller than that found in the January months considered in the present study. However, Clapp has suggested that his values are probably underestimates due to the too small heating maximum (-8×10^{-4} kj t^{-1} sec^{-1}) which he obtained at 38° N and also due to the fact that the vertical resolution of the correlation between heating and temperature on pressure surfaces was poor. The former explanation is substantiated to some extent by the results obtained by DAVIS (1963) using the heat-balance method also. He obtained an average January maximum value of $+53 \times 10^{-4}$ kj t^{-1} sec^{-1} in the 30–40° N latitude belt for the same layer.

In the case of the eddy component discrepancy it should be emphasized that the results of the present study indicate that the eddy generation is strongly dependent upon the characteristic time scale of the traveling eddies. As was seen in the present study, the covariances of the temperature and heating of the eddies was less negative when the monthly averaged fields rather than the daily patterns were considered. In fact, the covariances became positive in the cases of the spring and fall months ($G_A^{(e)}$ column M of Table 1). The fact that $G_A^{(z)}$ was closely approximated by the monthly average fields indicates a much larger characteristic time scale for the zonal patterns. This appears reasonable.

If we consider that the nine months considered here are sufficiently representative for obtaining an annual average, we obtain a value for the zonal generation of available potential energy of $+19 \times 10^{-4}$ kj m^{-2} sec^{-1} and a value for the eddy generation of -9×10^{-4} kj m^{-2} sec^{-1}. An appreciation for the value of the net generation of 10×10^{-4} kj m^{-2} sec^{-1} may be obtained by comparing this with the estimate of frictional dissipation obtained by Brunt (1939) of 50×10^{-4} kj m^{-2} sec^{-1} and by Pisharoty (1955) of 20×10^{-4} kj m^{-2} sec^{-1}.

It was felt that the data time-averaging procedure which was used in calculating the daily heaing patterns might tend to be damaging. (See Section 2*a* above.) The procedure was altered by considering only two sets of original analyses with adjacent map-times. The calculations were repeated for January 1962. The resulting monthly averages of $G_A^{(z)}$ and $G_A^{(e)}$ in units of 10^{-4} kj m^{-2} sec^{-1} were $+37$ and -15. Thus these average monthly values for January 1962 differ only slightly from those given in column D of Table 1.

The results of the present investigation indicate that the differential heating between high and low latitudes results in a positive generation of zonal available potential energy. The average for the three winter months considered ($+38 \times 10^{-4}$ kj m^{-2} sec^{-1}) was an order of magnitude less than that found in the two summer months ($+3 \times 10^{-4}$ kj m^{-2} sec^{-1}). The average value in spring was $+14 \times 10^{-4}$ kj m^{-2} sec^{-1} while that in fall was $+22 \times 10^{-4}$ kj m^{-2} sec^{-1}. As has been suggested by Lorenz (1954) the zonal available energy increases such that the strengthened thermal gradients lead to baroclinic instability and the growth of eddies. As northward heat transport increases to relieve the latitudinal thermal gradients, energy is converted from zonal potential to eddy potential energy. Part of the eddy potential component is converted to eddy kinetic energy through direct thermal circulations occurring in the cyclones and anticyclones. Lorenz has furthermore deduced that a portion of the eddy available potential energy is probably destroyed by diabatic processes—air masses which are relatively warm are cooled and those which are relatively cool are warmed. The results in the present study indicate that this is the case for all seasons except summer. The average values for the eddy generation of available potential energy in units of 10^{-4} kj m^{-2} sec^{-1} was: -24 for January, -8 for April, $+1$ for July and -7 for October. Thus for the eddies there is a tendency for the thermal gradients to be weakened by diabatic heating effects in all months considered except July.

In the future efforts should be made to improve upon the method of estimating the heating fields with particular emphasis on obtaining some estimates of the vertical distribution of the diabatic heating.

5. Acknowledgements

The author would like to express his thanks to Dr. A. Wiin-Nielsen for his valuable suggestions and discussions during the course of this investigation. Furthermore I would like to acknowledge the assistance of Dr. George Cressman of the National Meteorological Center who made the geopotential height analyses available.

REFERENCES

Berkofsky, L., and Bertoni, E. A., 1955, Mean topographic charts for the entire earth. *Bulletin of the American Meteorological Society*, **36**, No. 7, pp. 350–354.

Brunt, D., 1939, *Physical and Dynamical Meteorology*. Cambridge, England, Cambridge University Press, 428 p.

Budyko, M. I., 1956, *The Heat Balance of the Earth's Surface*. Leningrad, Gidrometeorologischeskoe izdatel'sto, 255 p.

Clapp, Phillip F., 1961, Normal heat sources and sinks in the lower troposphere in winter. *Monthly Weather Review*, **89**, No. 5, pp. 147–162.

Cressman, G. P., 1959, An operational objective analysis system. *Monthly Weather Review*, **87**, No. 10, pp. 367–374.

Cressman, G. P., 1960, Improved terrain effects in barotropic forecasts. *Monthly Weather Review*, **88**, pp. 327–342.

Davis, Paul, A., 1963, An analysis of the atmospheric heat budget. *Journal of Atmospheric Sciences*, **20**, No. 1, pp. 5–22.

Houghton, H. G., 1954, On the annual heat balance of the northern hemisphere. *Journal of Meteorology*, **11**, No. 1, pp. 1–9.

London, J., 1957, A Study of the Atmospheric Heat Balance, Final Report on contract AF 19(122)-165, (AFCRC-TR-57-287), New York University, Dept. of Meteorology and Oceanography, 99 pp.

Lorenz, E. N., 1954, The basis for a theory of the general circulation, Section IV of *Studies of the Atmospheric General Circulation*, Final Report Part I, General Circulation Project, Contract AF19(122)-153, Dept. of Meteorology, Massachusetts Institute of Technology, pp. 522–534.

Lorenz, E. N., 1955, Available potential energy and the maintenance of the general circulation. *Tellus*, **7**, No. 2, pp. 157–167.

Margules, M., 1903, Über die Energie der Stürme, *Jahrb. kais-kön Zent. für Met.*, Vienna. Translation by C. Abbe in *Smithson. Misc. Coll.*, **51**, 1910.

Pisharoty, P. R., 1955, The kinetic energy of the atmosphere, Article XIV in *Final Report*, Contract AF 19(122)-48, Dept. of Meteorology, University of California at Los Angeles.

Smagorinsky, J., 1963, General circulation experiments with the primitive equations. I. The basic experiment. *Monthly Weather Review*, **91**, No. 3, pp. 99–165.

Suomi, V. E., and Shen, W. C., 1963, Horizontal variation of infrared cooling and the generation of eddy available potential energy. *Journal of the Atmospheric Sciences*, **20**, No. 1, pp. 62–65.

Wiin-Nielsen, A., 1959, A study of energy conversion and meridional circulation for the large-scale motion in the atmosphere. *Monthly Weather Review*, **87**, pp. 319–332.

Wiin-Nielsen, A., and Brown, J. A., 1960, On diagnostic computations of atmospheric heat sources and sinks and the generation of available potential energy. *Proceedings of the International Symposium on Numerical Weather Prediction, Nov.* **7–13**, '**60** pp. 593–613.

Wiin-Nielsen, A., Brown, J. A., and Drake, M., 1963, On atmospheric energy conversions between the zonal flow and the eddies. *Tellus*, **15**, No. 3, pp. 261–279.